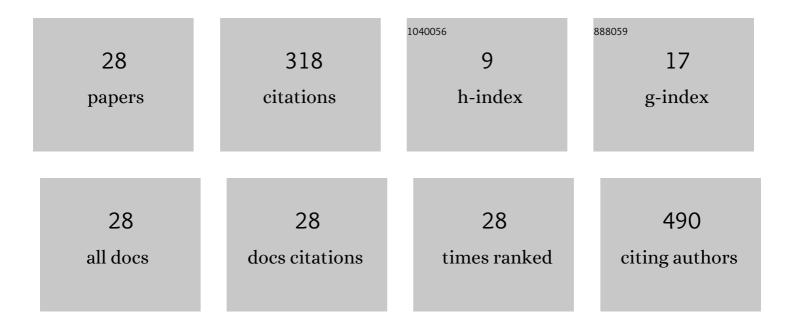
## Jerome Carnis

List of Publications by Year in descending order

Source: https://exaly.com/author-pdf/1086652/publications.pdf Version: 2024-02-01



LEDOME CADNUS

#	Article	IF	CITATIONS
1	Spatially resolved fluorescence of caesium lead halide perovskite supercrystals reveals quasi-atomic behavior of nanocrystals. Nature Communications, 2022, 13, 892.	12.8	15
2	Imaging the facet surface strain state of supported multi-faceted Pt nanoparticles during reaction. Nature Communications, 2022, 13, .	12.8	11
3	Robust ptychographic X-ray speckle tracking with multilayer Laue lenses. Optics Express, 2022, 30, 25450.	3.4	1
4	<i>P</i> recise wavefront characterization of x-ray optical elements using a laboratory source. Review of Scientific Instruments, 2022, 93, 073704.	1.3	1
5	<i>Gwaihir</i> : <i>Jupyter Notebook</i> graphical user interface for Bragg coherent diffraction imaging. Journal of Applied Crystallography, 2022, 55, 1045-1054.	4.5	1
6	Facetâ€Dependent Strain Determination in Electrochemically Synthetized Platinum Model Catalytic Nanoparticles. Small, 2021, 17, e2007702.	10.0	4
7	High spatial coherence and short pulse duration revealed by the Hanbury Brown and Twiss interferometry at the European XFEL. Structural Dynamics, 2021, 8, 044305.	2.3	9
8	Twin boundary migration in an individual platinum nanocrystal during catalytic CO oxidation. Nature Communications, 2021, 12, 5385.	12.8	14
9	Single alloy nanoparticle x-ray imaging during a catalytic reaction. Science Advances, 2021, 7, eabh0757.	10.3	7
10	Exploring the 3D structure and defects of a self-assembled gold mesocrystal by coherent X-ray diffraction imaging. Nanoscale, 2021, 13, 10425-10435.	5.6	8
11	Morphogenesis of Magnetite Mesocrystals: Interplay between Nanoparticle Morphology and Solvation Shell. Chemistry of Materials, 2021, 33, 9119-9130.	6.7	11
12	Time-resolved in situ visualization of the structural response of zeolites during catalysis. Nature Communications, 2020, 11, 5901.	12.8	11
13	Mapping Inversion Domain Boundaries along Single GaN Wires with Bragg Coherent X-ray Imaging. ACS Nano, 2020, 14, 10305-10312.	14.6	8
14	<i>PyNX</i> : high-performance computing toolkit for coherent X-ray imaging based on operators. Journal of Applied Crystallography, 2020, 53, 1404-1413.	4.5	38
15	Continuous scanning for Bragg coherent X-ray imaging. Scientific Reports, 2020, 10, 12760.	3.3	6
16	Cylindrical Reflex Triode Warm X-Ray Source. IEEE Transactions on Plasma Science, 2020, 48, 3877-3889.	1.3	6
17	Variableâ€Wavelength Quick Scanning Nanofocused Xâ€Ray Microscopy for In Situ Strain and Tilt Mapping. Small, 2020, 16, 1905990.	10.0	3
18	Surface and Interfacial Morphology of Bulk Heterojunction Layers in Organic Solar Cells with Solvent Additive. Journal of the Korean Physical Society, 2019, 75, 498-502.	0.7	0

JEROME CARNIS

#	Article	IF	CITATIONS
19	<i>In situ</i> structural evolution of single particle model catalysts under ambient pressure reaction conditions Nanoscale, 2019, 11, 331-338 Advanced Coherent X-ray Diffraction and Electron Microscopy of Individual <mml:math< td=""><td>5.6</td><td>10</td></mml:math<>	5.6	10
20	xmins:mml="http://www.w3.org/1998/Math/MathML" display="inline" overflow="scroll"> <mml:mrow><mml:mi>In</mml:mi><mml:mi mathvariant="normal"&gt;P</mml:mi </mml:mrow> Nanocrystals on <mml:math xmlns:mml="http://www.w3.org/1998/Math/MathML" display="inline"</mml:math 	3.8	2
21	overflow="scroll"> <mml:mi>Si</mml:mi> Nanotips for III-V-on- <mml:math mlns:mml="ht Electrode-induced lattice distortions in GaAs multi-quantum-dot arrays. Journal of Materials Research, 2019, 34, 1291-1301.</mml:math 	2.6	2
22	Towards a quantitative determination of strain in Bragg Coherent X-ray Diffraction Imaging: artefacts and sign convention in reconstructions. Scientific Reports, 2019, 9, 17357.	3.3	23
23	Crystallographic orientation of facets and planar defects in functional nanostructures elucidated by nano-focused coherent diffractive X-ray imaging. Nanoscale, 2018, 10, 4833-4840.	5.6	14
24	Active site localization of methane oxidation on Pt nanocrystals. Nature Communications, 2018, 9, 3422.	12.8	58
25	Demonstration of Feasibility of X-Ray Free Electron Laser Studies of Dynamics of Nanoparticles in Entangled Polymer Melts. Scientific Reports, 2014, 4, 6017.	3.3	41
26	Coherent X-ray scattering beamline at port 9C ofÂPohang Light Source II. Journal of Synchrotron Radiation, 2014, 21, 264-267.	2.4	9
27	Visualization of photogeneration transport characteristics of a pentacene thin-film transistor at selected wavelengths. Thin Solid Films, 2013, 534, 503-507.	1.8	3
28	Characterization of the field-effect conductivity distribution in pentacene thin-film transistors by a near-field scanning microwave microscope. Synthetic Metals, 2011, 161, 931-936.	3.9	2